

# Influence of sodium chromate and dodecylamine on enhanced dissolution behavior of Cu–Ni alloy induced by AFM tip scratching

JUN-E QU

*Department of Chemistry, HuaZhong University of Science and Technology, Wuhan 430074, People's Republic of China; School of Chemistry and Material Science, Hubei University, Wuhan 430062, China*

XINGPENG GUO\*, ZHENYU CHEN

*Department of Chemistry, HuaZhong University of Science and Technology, Wuhan 430074, People's Republic of China  
E-mail: guoxp@mail.hust.edu.cn*

**Published online:** 21 April 2006

The influence of two inhibitors sodium chromate and dodecylamine on enhanced dissolution of Cu–Ni alloy initiated by atomic force microscopy (AFM) tip scratching in 1.5 M NaCl and 0.01 M HCl was investigated. The lateral force traces and force versus distance curves were measured by AFM in distilled water without or with inhibitors to investigate the influence of inhibitors on physical characters of sample surfaces. The results indicated that enhanced dissolution caused by AFM tip scratching was inhibited by adding sodium chromate or dodecylamine into the corrosive solutions, but their inhibition mechanisms are different. The inhibition effect of sodium chromate is due to its oxidation ability to repair the destroyed protection film and the increase of rigidity of metal surface resulted from the formation of oxide film containing Cr elements. On the other hand, the inhibition effect of dodecylamine is due to the organic adsorption film on metal surface to weaken the friction forces between the tip and the sample and to elevate the ionization energy of metal. © 2006 Springer Science + Business Media, Inc.

## 1. Introduction

During the imaging by AFM in contact mode, the forces between the tip and the sample are small so that there is almost no damage to rigid samples, but continuous scanning with strong force loaded on the tip may affect the surface status. AFM tip scratching can be utilized to investigate the corrosion behavior of metal at different force conditions. For example, the research of Guay [1] and Frankel [2, 3] showed that the dissolution rate of aluminum or aluminum alloy could be locally enhanced during controlled AFM scanning in NaCl solutions.

When the AFM tip scans over the sample surface, the tip experiences forces both in vertical and lateral directions. The vertical interaction between the tip and the sample can be obtained from the force-distance (F-D) curve by detecting the vertical deflection of the cantilever [4]. The degree of the cantilever's torsion in the lateral direction can also be measured, which reflects the friction interac-

tion between the tip and the sample surface. The lateral friction force is obtained commonly by frictional loop test [5, 6]. F-D curve and frictional loop test provide feasible methods to investigate the micro physical characterization of the sample surface in nanometer scale.

Chromate is a kind of inorganic corrosion inhibitor for Cu [7], and some organic compounds containing amidocyanogens have the ability to inhibit the corrosion of Cu [8, 9]. In this work, sodium chromate and the simple structured dodecylamine have been used as inhibitors. Their inhibition action on corrosion behavior of Cu–Ni alloy in 1.5 M NaCl and 0.01 M HCl was investigated by polarization curves, and then as the emphasis of our work, the dissolution behavior of Cu–Ni alloy initiated by AFM tip scratching in 1.5 M NaCl and 0.01 M HCl solutions without or with inhibitors was investigated. F-D curve measurements were performed to study the effect of Na<sub>2</sub>CrO<sub>4</sub> on the rigidity of sample surface, and

\* Author to whom all correspondence should be addressed.

frictional force curve tests were carried out to investigate the effect of dodecylamine on tip-sample interaction. Their inhibition mechanisms on accelerated dissolution of Cu–Ni alloy in the scratched areas were discussed.

## 2. Experimental

The corrosive solutions 1.5 M NaCl and 0.01 M HCl were prepared with distilled water. Dodecylamine (98%, Acro) and sodium chromate (analytic pure) were used as received. The metal materials were copper-nickel alloy foils with composition of (wt%): Cu base, Ni 40.68, Mn 1.54, P 5.91, S 0.16, Mg 0.02, Fe 0.29, Si 0.04, Zn 0.02. The samples were wet ground through 1200 grit SiC paper, rinsed with distilled water, degreased with ethanol, and immediately used for potentiodynamic polarization. For AFM measurements, a polishing process on cloth wheels using diamond paste to 0.5  $\mu\text{m}$  was performed for the alloy samples following the grinding process by SiC papers, and then they were rinsed with distilled water, treated with supersonic cleaning in ethanol, and stored in air before test.

The polarization curves were recorded from  $-400$  to  $+400$  mV relative to the corrosion potential ( $E_{\text{corr}}$ ) with a scan speed of 1 mV/s in the test solutions without or with inhibitors by an IM6e electrochemical workstation, using a standard three electrode configuration with a saturated calomel reference electrode and a platinum counter electrode.

Scratching experiments were performed with a SPA400 AFM (Seiko Instruments Inc.) in contact mode using commercial Si cantilevers with spring constant of 3 N/m. An open electrolyte cell with a volume of 1.5 ml was used for the *in situ* experiments. Considering that the scratching might damage the tip, every scratching experiment was done by a new tip.

The F-D curve measurements were performed in distilled water with and without  $\text{Na}_2\text{CrO}_4$  and the frictional loop tests in distilled water with and without dodecylamine. The F-D curves were recorded from the vertical distance 1000 to  $-50$  nm using Si cantilever with spring constant of 20 N/m. The frictional loops were obtained by recording traces of cantilever lateral deflection using Si cantilever with spring constant of 3 N/m, while the sample was scanned back and forth over 58  $\mu\text{m}$  distances.

## 3. Results and discussion

### 3.1. Polarization curves

Potentiodynamic polarization curves for Cu–Ni alloy in 1.5 M NaCl and 0.01 M HCl without or with inhibitors are shown in Fig. 1. A protective film containing  $\text{Cu}_2\text{O}$ ,  $\text{CuO}$ ,  $\text{CuCO}_3 \cdot \text{Cu}(\text{OH})_2$ ,  $\text{NiO}$  etc. is formed on Cu–Ni alloy in air condition spontaneously, and in solutions containing aggressive anions, pitting corrosion or intergranular corrosion tends to occur after an induction period [10]. If the solution is acidic, the film becomes unstable and can

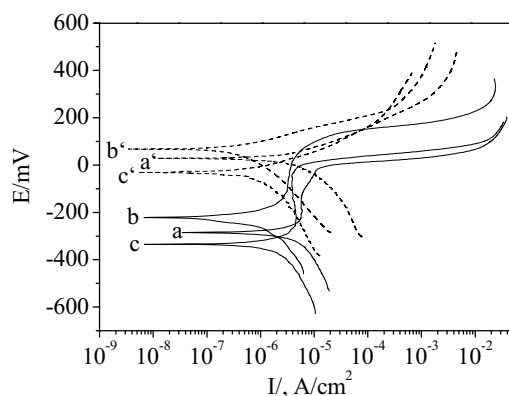


Figure 1 Potentiodynamic polarization curves for Cu–Ni alloy in: (a) 1.5 M NaCl; (b) 1.5 M NaCl + 0.005 M  $\text{Na}_2\text{CrO}_4$ ; (c) 1.5 M NaCl + 0.005 M dodecylamine; (a') 0.01 M HCl; (b') 0.01 M HCl + 0.005 M  $\text{Na}_2\text{CrO}_4$ ; and (c') 0.01 M HCl + 0.005 M dodecylamine.

be chemically dissolved. So as shown in the polarization curves in Fig. 1, passivation plateau is observed in anodic polarization region in NaCl in stead of active anodic dissolution curve in HCl.

The parameters obtained from polarization curves in NaCl and HCl are respectively listed in Tables I and II, where  $E_{\text{corr}}$  is corrosion potential,  $E_b$  break through potential,  $i_p$  passive current density,  $\beta_a$  apparent anodic Tafel slope,  $\beta_c$  apparent cathodic Tafel slope,  $i_c$  corrosion current density deduced from cathodic polarization curves, and  $\eta\%$  the percentage inhibition efficiency.  $\eta\%$  is calculated from equation [ $\eta\% = (i_{c,\text{un}} - i_{c,\text{inh}})/i_{c,\text{un}}$ ], where  $i_{c,\text{un}}$ ,  $i_{c,\text{inh}}$  are corrosion current density in the absence of inhibitor and in the presence of inhibitor.

It is clear that adding of  $\text{Na}_2\text{CrO}_4$  and dodecylamine made  $E_c$  shift to positive and negative direction, respectively. This implies  $\text{Na}_2\text{CrO}_4$  was more pronounced on the anodic reaction and dodecylamine was more pronounced on the cathodic reaction. In both NaCl and HCl solutions, the inhibition efficiency of  $\text{Na}_2\text{CrO}_4$  was more notable comparing with dodecylamine. And especially in NaCl the presence of  $\text{Na}_2\text{CrO}_4$  promoted to form a more compact protective film, making  $E_b$  shift to positive direction and  $i_p$  decrease remarkably.

### 3.2. Enhanced dissolution induced by AFM tip scratching

After 30 min immersion in the corrosive solutions, the AFM tip was controlled to scan over a  $4 \times 4 \mu\text{m}^2$  area continuously for 30 min with load of 750 nN. Then the topographical image of an  $8 \times 8 \mu\text{m}^2$  area containing the central scratched district was measured. The images obtained in 1.5 M NaCl and in 0.01 M HCl are shown in Fig. 2a and b respectively.

It can be distinguished from Fig. 2 that square holes were produced in the scratched areas, and the depths of which in NaCl and HCl solutions were about 35 and 80 nm respectively. In NaCl solution, the nicks produced

TABLE I Polarization parameters for Cu–Ni alloy in 1.5 M NaCl without and with addition of an inhibitor at a concentration of 0.005 M

Inhibitor	$E_{\text{corr}}$ (mV)	$E_b$ (mV)	$i_p$ (A/cm <sup>2</sup> )	$\beta_c$ (mV/dec)	$i_c$ (A/cm <sup>2</sup> )	$\eta$ (%)
Blank	–284	–53	6.33 e-6	405	3.27 e-7	–
Sodium chromate	–221	100	3.10 e-6	299	1.38 e-8	96
Dodecylamine	–335	15	3.64 e-6	391	1.14 e-7	65

TABLE II Polarization parameters for Cu–Ni alloy in 0.01 M HCl without and with addition of an inhibitor at a concentration of 0.005 M

Inhibitor	$E_{\text{corr}}$ (mV)	$\beta_a$ (mV/dec)	$\beta_c$ (mV/dec)	$i_c$ (A/cm <sup>2</sup> )	$\eta$ (%)
Blank	–42	106	297	2.30 e-7	–
Sodium chromate	–2	57	126	1.01 e-8	96
Dodecylamine	–91	61	117	7.81 e-8	66

in the polishing process were still differentiable on the unscratched area around the hole as shown in Fig. 2a. But in HCl solution, distinct dissolution took place on the unscratched area as shown in Fig. 2b. The experiment results show that in HCl both the natural corrosion in the unscratched area and the enhanced dissolution in the scratched area were more severe than that observed in NaCl. However, when the load was much lower (such as 50 nN), the enhanced dissolution of alloy induced by the scratching was much slighter and the difference in height between the scratched and unscratched areas could hardly be quantitatively described. This result implied that tip-induced churning is not a main factor for enhanced dissolution.

In the research of Guay *et al.* [1], enhanced dissolution of thin aluminum film was observed in NaCl solution. They deduced that while the tip continuously scanned over the aluminum surface, the friction forces between the tip and the sample caused local heating of the substrate which provided enough energy to overcome the activation barrier for the chemical reaction of the chloride anion with the aluminum ion to form a soluble complex product, so the breakdown of aluminum oxide film and dissolution of the substrate were accelerated. And Frankel *et al.* [2] interpreted the formation of uniform smooth-bottom trench obtained in the scratched area of AA1100 samples in NaCl solution as the process of surface depassivation caused by

the AFM tip scratching, followed by limited dissolution and repassivation.

The results in this work show that, scratched by AFM tip in corrosive solution, Cu–Ni alloy has the similar accelerated dissolution behavior as aluminum and aluminum alloy. This implies that chemical combination of Cl anions with the Cu and/or Ni cations can be enhanced by tip scratching also. Moreover the tip might mechanically scratch away the surface of the alloy [3]. While in NaCl solution, the mechanical destroy leads to reduplicate effects for enhanced dissolution, one is the depassivation of the protective film, and the other is the losing of the alloy base. For alloy in HCl solution, the passive film is unstable and can be chemically dissolved, so the mechanical destroy mainly leads to the losing of the alloy base. The composite influence of these factors resulted in the enhanced dissolution of the scratched areas.

While the alloy exposed to NaCl, repassivation and depassivation of the destroyed surface coexisted. But in HCl the protective is nonexistent after being chemically dissolved, furthermore the chemical dissolution of the oxide film exposes the metal base to the solution, which suffers from electrochemical corrosion. So as a total result, both the natural corrosion in unscratched area and accelerated dissolution in scratched area in HCl solution are more severe than that in NaCl solution.

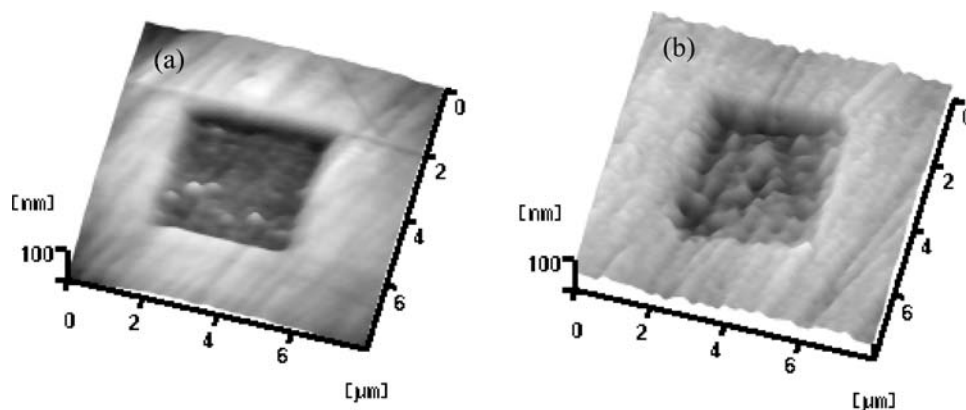


Figure 2 The corrosion topographic images of Cu–Ni alloy obtained in: (a) 1.5 M NaCl; and (b) 0.01 M HCl.

### 3.3. The inhibition of accelerated dissolution by sodium chromate

The same scratching experiments were performed in 1.5 M NaCl and 0.01 M HCl solutions in the presence of 0.005 M Na<sub>2</sub>CrO<sub>4</sub>, and the topographical images measured on the surfaces of 8 × 8 μm<sup>2</sup> size containing the central scratched areas of 4 × 4 μm<sup>2</sup> after 30 min scratching are shown in Fig. 3a and b.

In 1.5 M NaCl containing 0.005 M Na<sub>2</sub>CrO<sub>4</sub>, no hole as in Fig. 2a was observed, but some scars caused by tip scratching were presented in the scratched area. In 0.01 M HCl containing 0.005 M Na<sub>2</sub>CrO<sub>4</sub>, a hole with depth of about 20 nm was produced in the scratched area, which is only about a quarter of the depth of that produced in blank HCl solution as shown in Fig. 2b. That means, as a corrosion inhibitor in NaCl and HCl for Cu—Ni alloy, Na<sub>2</sub>CrO<sub>4</sub> suppressed the enhanced dissolution caused by tip scratching, and its inhibition effect was much better in NaCl solution than in HCl solution.

Frankel *et al.* [2] found that when the concentration of Na<sub>2</sub>CrO<sub>7</sub> in 0.5 M NaCl solutions increased from 0.0001 M to 0.5 M, the inhibition effect for accelerated dissolution in scratched surface of pure aluminum (99.99%) became more remarkable. The inhibition mechanism was proposed in two aspects by the authors: One was concerned with the protective film formed owing to the oxidation ability of Na<sub>2</sub>CrO<sub>7</sub> that inhibited the corrosion process; the other was concerned with the oxide and

hydrate containing chrome element formed on the alloy surface that made the stiffness of the surface increased to restrain the mechanical destroy caused by scratching. But no direct evidence has been provided in their work to testify the alteration of the surface stiffness.

Different surfaces, as a result of fabrication and other treatments, have different values of Young's modulus. It has been reported that the slope of the AFM F-D curve after the contact point of the tip with the surface is related to the stiffness and elastic modulus of the surface during atomic force measurements, and the higher the slope value is, the harder the surface is [11].

SERS (surface enhanced raman scattering) studies of McCreery *et al.* [12] has proved that a Cr<sup>III</sup> oxyhydroxide film is formed on copper surface exposed to chromate. In this work the alteration of the surface stiffness of Cu—Ni alloy was validated by determining the slope of the F-D curve. To get obvious contrast, the concentration of Na<sub>2</sub>CrO<sub>4</sub> was chosen as 0.5 M. The F-D curves were measured in blank distilled water and at 1, 2, and 3 h time after Na<sub>2</sub>CrO<sub>4</sub> was added to the distilled water. The representative curves are displaced in Fig. 4a. Ten F-D curves were acquired at each defined time, and the averaged slope was calculated out from the section of the curves after the contact point of the tip with the surface for both cases of the approaching and retracting of the AFM tip. The time-dependent changes of the F-D slope (*S*<sub>F-D</sub>) are displayed in Fig. 4b. The results show that the slope of the

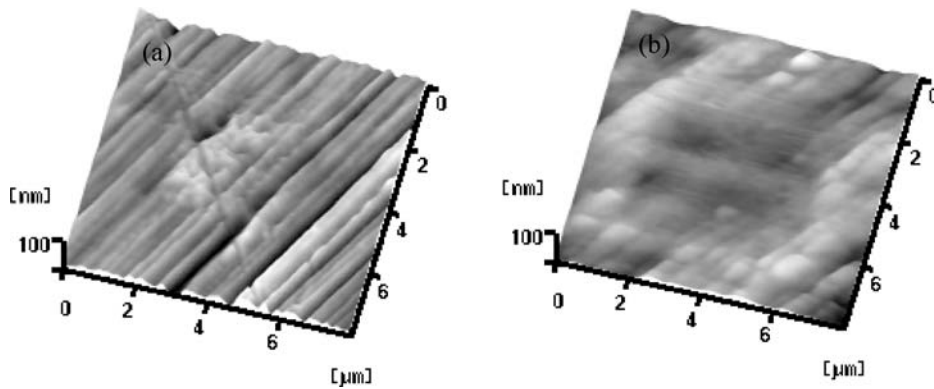


Figure 3 The corrosion topographic images of Cu—Ni alloy obtained in: (a) 1.5 M NaCl + 0.005 M Na<sub>2</sub>CrO<sub>4</sub>; and in 0.01 M HCl + 0.005 M Na<sub>2</sub>CrO<sub>4</sub> (b).

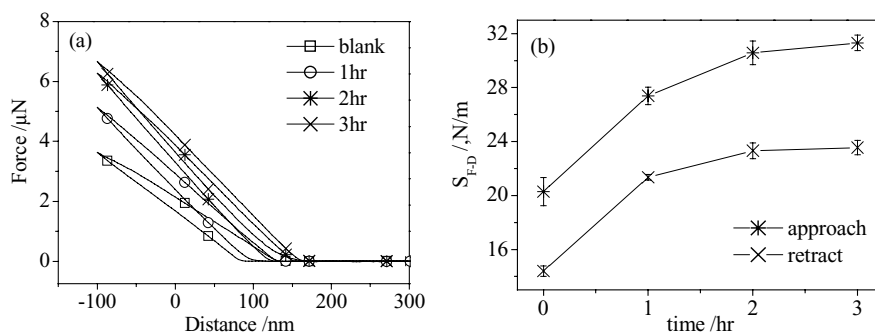


Figure 4 The effect of Na<sub>2</sub>CrO<sub>4</sub> on the F-D curves: (a) F-D curves obtained in different time; (b) The time-dependent changes of F-D curve's slope.

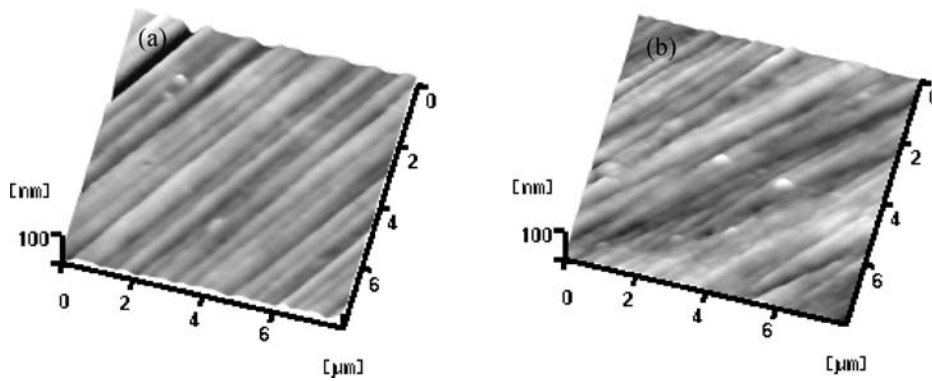


Figure 5 The corrosion topographic images of Cu–Ni alloy in: (a) 1.5 M NaCl + 0.005 M dodecylamine; (b) 0.01 M HCl + 0.005 M dodecylamine.

F-D curves increased rapidly in the first two hours. This implies that the alloy surface was oxidized rapidly after contacting with oxidant  $\text{Na}_2\text{CrO}_4$ , which made the surface stiffness increased rapidly. After 2 h time, the protective oxide film had been formed so that the increasing rate of the stiffness became slower.

The results mentioned above imply that the protective film formed by the oxidation action of  $\text{Na}_2\text{CrO}_4$  reduces the corrosion process and the higher rigidity of the surface film containing Cr suppresses the mechanical destruction of the surface. A competition existed between the destruction and repair processes during the scratching, so that the scratched area in NaCl solution exhibited some scars, having dissimilar topography from the surrounding area. In HCl solution, owing to the chemical dissolution of oxide film, the inhibition effect of  $\text{Na}_2\text{CrO}_4$  on the accelerated dissolution was weaker than that in NaCl solution, so there was still a pit formed on the central scratched area.

### 3.4. The inhibition of accelerated dissolution by dodecylamine

The scratching experiments were also carried out in 1.5 M NaCl and 0.01 M HCl solutions containing 0.005 M dode-

cylamine. The topographical images measured on the surfaces of  $8 \times 8 \mu\text{m}^2$  size containing the central scratched areas of  $4 \times 4 \mu\text{m}^2$  after 30 min scratching are shown in Fig. 5a and b.

In both solutions, no holes as that in Fig. 2 were observed and the topographical images of scratched areas in the central did not present distinct differences from that of unscratched areas, meaning that as a corrosion inhibitor in NaCl and HCl for Cu–Ni alloy, dodecylamine suppressed the enhanced dissolution caused by tip scratching and its inhibition effect is more notable than  $\text{Na}_2\text{CrO}_4$  especially in HCl solution.

It was found that some kinds of self-assembled monolayers (SAMS) exhibiting high hydrophobicity and low surface energies could be used as lubrication to suppress the frictional interaction and abrasion [13]. For the molecules of organic corrosion inhibitor adsorbed on metal surface, their hydrophobic alkyl chains are arranged towards the solution to form a hydrophobic interface. So we can imagine adsorption film of organic corrosion inhibitor on the metal surface should have the action as lubrication when the AFM tip scans over the metal surface.

The frictional loop acquired with tip load of 750 nN in distilled water is shown in Fig. 6a, and that acquired at the

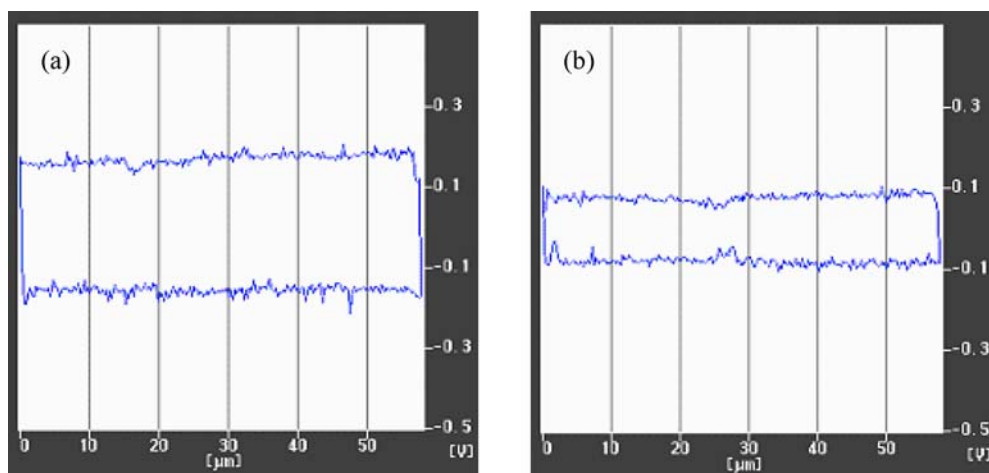


Figure 6 The frictional loops between the tip and the sample: (a) with load of 750 nN, acquired in distilled water; (b) with load of 750 nN, acquired at the time when the dodecylamine has been added to the distilled water for 120 min.



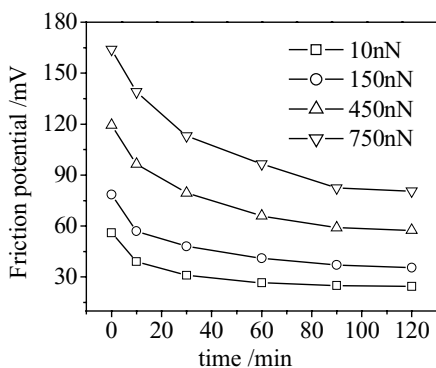


Figure 7 Dependence of frictional potential on time at different tip loads.

time when dodecylamine has been added into the distilled water for 120 min is shown in Fig. 6b. For each frictional loop, continuous scans of 5 times were performed and the computer gave out an averaged frictional loop curve automatically. The absolute values of friction forces are not given in the curves, and the relative values of friction forces can be reflected by the values of friction potential. The higher the value of the potential, the greater the value of the friction force [14]. It can be discovered from Fig. 5 that after dodecylamine having been added to the distilled water for 120 min, the friction force between the tip and the sample surface was diminished obviously.

The relationship between the frictional potential and the elapsed time after adding dodecylamine to the distilled water at different tip load values (10, 150, 450 and 750 nN) deduced from all the measured frictional loops is displayed in Fig. 7. It can be discovered that at the same time point, the friction force was increased with the increasing of the load. The reason should be that larger load on the tip would make the sheared resistance increased. It has the same trend at each load value that friction potential was decreased with the time evolution and approached a constant after the time of about 90 min, implying that the adsorption balance of dodecylamine on Cu—Ni alloy was reached after 90 min. In the initial time, the inhibitor molecules adsorbed onto the sample surface rapidly, and the density of the adsorption film was increased continuously, as a result the frictional interaction between the tip and the sample was decreased gradually. With the time evolution, the saturated adsorption of inhibition film was approached, so the values of frictional force tended to be invariable.

The differential capacitance curve tests had been performed in our previous work and proved that the surface of corroded Cu—Ni alloy in NaCl solution has extra negative charges [15]. After adding dodecylamine to the solutions, the polar amidocyanogen is combined with the hydrogen ion ionized from the H<sub>2</sub>O molecule to form (C<sub>12</sub>H<sub>23</sub>NH<sub>3</sub>)<sup>+</sup>, and the positive charged dodecylamine molecules are easy to be physically adsorbed onto the negative charged surface. Meanwhile there exists chemical adsorption of polar amidocyanogens on the copper-nickel alloy surface with the hydrophobic alkyl chains arranged towards the solution [8]. When the AFM

tip moves close to the surface it will encounter space resistance. This space resistance and the physical existence of the adsorption film will reduce the probability of direct frictional interaction between the tip and the sample surface. The local heating of the substrate arising from the frictional interaction is suppressed, so not enough convertible energy can be offered to activate the chemical reaction of the chloride anions with the metal cations, and the mechanical breakdown of the protective film is also remarkably reduced. On the other hand, the structure alteration of double-electric layer caused by the adsorption of the polar amidocyanogens on the metal surface can heighten the activation energy for metal ionization [16]. As a total result, the accelerated dissolution of copper-nickel alloy induced by tip scratching is suppressed.

#### 4. Conclusions

1. The result of potentiodynamic polarization curves showed that Na<sub>2</sub>CrO<sub>4</sub> and dodecylamine both have inhibition effect on corrosion of Cu—Ni alloy in 1.5 M NaCl and 0.01 M HCl.
2. AFM tip scratching made the dissolution of Cu—Ni alloy in 1.5 M NaCl and 0.01 M HCl solutions enhanced. Both the natural corrosion on unscratched area and enhanced dissolution in scratched area were more severe in HCl solution than that in NaCl solution.
3. Adding Na<sub>2</sub>CrO<sub>4</sub> to NaCl and HCl solutions made the enhanced dissolution of copper-nickel alloy induced by tip scratching suppressed. For sodium chromate, the inhibition was due to its oxidation ability to repair the destroyed protection films and the increase of rigidity of metal surfaces resulted from the formation of oxide films containing chromium elements.
4. Dodecylamine in the NaCl and HCl solutions has more effective inhibition action for accelerated dissolution induced by tip scratching than Na<sub>2</sub>CrO<sub>4</sub>. In this case, the decrease of friction forces between the tip and the sample and the elevation of ionization energy of metal caused by inhibitor's adsorption on metal surface make the enhanced dissolution reduced remarkably. This implies that some organic compounds such as dodecylamine can be used as inhibitors and lubricants to suppress the erosion corrosion and out-side force induced corrosion of metal in corrosive mediums.

#### Acknowledgment

This work was supported by National Natural Science Foundation of China (No 50471062).

#### Reference

1. L. CHEN and D. GUAY, *J. Electrochem. Soc.* **141** (1994) L43.
2. P. SCHUMUTZ and G. S. FRANKEL, *ibid.* **145** (1998) 2295.
3. *Idem.*, *ibid.* **146** (1999) 4461.
4. A. VINCKICR and G. SEMENZA, *FEBS Lett.* **430** (1998) 12.
5. V. DMITRI, N. ALEKSANDR, F. R. LAWRENCE and M. L. CHARIES, *J. Am. Chem. Soc.* **119** (1997) 2006.
6. G. S. WATSON, B. P. DINTÉ, J. A. BLACH-WATSON and S. MYHRA, *Appl. Surf. Sci.* **235** (2004) 38.

7. F. X. GAN, Z. X. DAI, D. H. WANG and L. A. YAO, *Chinese J. Appl. Chem.* **15** (1998) 45.
8. E. STUPNISEK-LISAC, A. BRNADA and A. D. MANCE, *Corros. Sci.* **42** (2000) 243.
9. S. T. YAO, X. Y. WU and Y. R. SUN, *J. Shenyang Univ. Technol.* **22** (2000) 173.
10. L. Y. LIN, S. F. LIU, Z. C. LIU and J. XU, *J. Corros. Sci. Protect. Technol.* **11** (1999) 37.
11. O. LENSCH, B. ENDERS, J. KNECHT and W. ENSINGER, *Nucl. Instrum. and Meth. in Phys. Res.* **B175-177** (2001) 683.
12. B. L. HURLEY and R. L. MCCREEY, *J. Electrochem. Soc.* **150** (2003) B367.
13. K. KOMVOPOULOUS, *Wear* **200** (1996) 305.
14. Y. H. YANG and M. L. ABRAHAM, *J. Coll. Interf. Sci.* **267** (2003) 352.
15. J.-E. QU, X. P. GUO and Z. Y. CHEN, *Mater. Chem. Phys.* **93** (2005) 388.
16. Y. P. YI, *J. Yichun Teach. Coll.* **21** (1999) 32.

*Received 27 April  
and accepted 24 August 2005*